

Research on sodium chloride solution sensing based on one-dimensional mirror photonic crystals

QINGSONG JIAN, JIANWEI WU*

College of Physics and Electronic Engineering, Chongqing Normal University, Chongqing, P.R. China

In this study, a one-dimensional mirror photonic crystal sensing model with GaN and AlN arranged alternately was designed to measure the concentration of NaCl solution using the transmission matrix method. The model is less affected by the ambient temperature, and the sensitivity reaches 1002 nm/RIU with a quality factor of 1990. In addition, the effects of the photonic crystal period number and the angle of incidence on the model are also investigated.

(Received June 3, 2024; accepted February 3, 2025)

Keywords: Photonic crystal, Transfer matrix method, Defect mode, Sodium chloride solution

1. Introduction

Controlling and manipulating the propagation of light is one of the active fields of research in optics and optoelectronics, and the propagation of waves in periodic structures has always been a subject of intensive study. With the development of quantum and fluctuating optics, people have begun to take great research interest in the control of photons, and seek to realize the transmission and processing of information through the control of photons. Photonic crystal as a periodic material with alternating dielectric constant, photons inside the crystal can be used as the propagation carrier of electromagnetic waves, and photons can replace electrons in semiconductors for information transmission. Photonic crystals have been widely studied by the scientific community since they were first discovered by virtue of their unique optical properties.

The development of photonic crystals was firstly proposed by Yablonovitch and John in 1987 [1-2], which are microstructured crystals formed by the periodic arrangement of dielectric materials with different refractive indices in space, and according to the different ways of the dielectric materials arranged in space, they are classified into one-dimensional photonic crystals (1D-PC), two-dimensional photonic crystals (2D-PC) and three-dimensional photonic crystals (3D-PC) [3]. The most important features of photonic crystals are photonic forbidden bands and photonic localization. Photonic forbidden bands control the motion of light inside the crystal and can prohibit the propagation of light of a specific frequency inside the crystal. Photonic localization, on the other hand, is a specific phenomenon caused by introducing defects or impurities into the photonic crystal structure, thus destroying its original

periodicity or symmetry, and mainly contains two modes, namely, defect mode [4-6] and surface state [7-9]. At present, the research on photonic crystal sensing mainly focuses on how to introduce functional materials as defects into the photonic crystal structure, and change the propagation of electromagnetic waves within the photonic bandgap through the stimulation of the environment on the functional materials, so as to realize the detection of different external stimulus responses. The common external stimuli are magnetic field, electric field, refractive index, virus, nucleic acid, antibody etc.

Due to the existence of a periodic arrangement of dielectric materials in only one direction and the simplicity and low cost of fabrication, the realization of sensing and identification of physical, chemical, and biological quantities based on one-dimensional photonic crystals has been widely studied in recent decades and has become one of the popular structures to realize a wide range of applications [10]. Wan et al. proposed a one-dimensional photonic crystal sensor based on the resonance of a defect mode, and introduced the plasma as a defect into the photonic crystal structure, realizing the simultaneous measurement of four physical quantities: magnetic induction strength, plasma density, refractive index, and angle of incidence [11]. Arafa et al. designed a defective photonic crystal sensing model to realize the detection of poliovirus concentration, and the sensitivity of the structure was as high as 1189 nm/RIU [12]. Zaky et al. proposed a one-dimensional photonic crystal sensing model of porous silicon doped with plasma, which can be used for the detection of hazardous greenhouse gases, and the structure effectively reduces the interference of the external magnetic field, and the sensitivity is as high as 16.35 Ghz/RIU, the quality factor and quality coefficient are at a high level [13]. Shiva et al.

coupled a one-dimensional photonic crystal with a plasma waveguide to construct a novel optical biosensing model that can be used to detect basal cancer cells, and the sensitivity of this model reached 718.6 nm/RIU [14]. Panda et al. designed a one-dimensional photonic crystal model utilizing a composite material, LiNbO₃, which can be used to detect the concentration of sucrose in aqueous solution. model has high sensitivity and low LOD [15].

As a widely used solution product in the medical field, the main component of saline is sodium chloride, and the concentration of sodium chloride in saline must be controlled to be comparable to that of blood. Meanwhile, in the process of desalination control, real-time monitoring of the sodium chloride concentration of the discharged water is required [16-17]. Therefore, the study of the real-time measurement of the concentration of sodium chloride solution is of great significance and application value.

In this study, we designed a one-dimensional mirror photonic crystal based on the alternating arrangement of gallium nitride and aluminum nitride, inserted the sodium chloride solution to be measured as a defective layer into the one-dimensional photonic crystal structure, calculated the transmission characteristics of the one-dimensional mirror photonic crystal by using the transmission matrix method, and established the relationship between the transmission wavelength and the concentration to be measured, realizing the real-time, non-contact, and accurate measurement of the sodium chloride concentration. Meanwhile, we also investigated the effects of photonic crystal period number and incident angle on the sensor, and optimized the structure of the sensor.

2. Structural model

Fig. 1 shows the designed one-dimensional defective photonic crystal model, which consists of two different dielectric materials alternating periodically, with a defective layer in the middle.

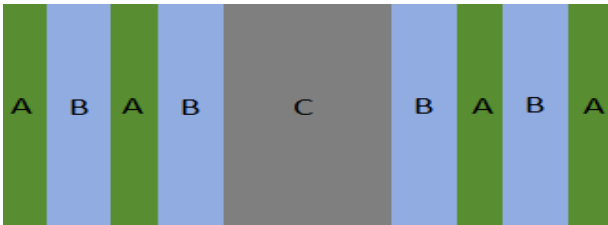


Fig. 1. Structural design of proposed 1d defective planar photonic crystal $(AB)^N C (BA)^N$ (colour online)

In order to obtain a photon forbidden band with a certain bandwidth, gallium nitride (GaN) is selected as the high refractive index component material, denoted as A; aluminum nitride (AlN) is selected as the low

refractive index component material, denoted as B, and the sodium chloride solution to be tested is selected as the material of the defect layer, denoted as C. Gallium nitride is a binary direct-band system semiconductor material with good thermal stability, and it can be stably operated under high temperature conditions. Gallium nitride has good resistance to chemical corrosion in the environment, which makes it maintain good performance in different solutions. At the same time, gallium nitride has many applications in the optical field, especially in ultraviolet detection and blue LED development, its preparation process is more mature, can significantly reduce the difficulty of manufacturing. Gallium nitride in the wavelength range of 0.35 μm - 10 μm its refractive index and wavelength dependence [18]:

$$n_A^2 = 3.1399 + \frac{13.786 \lambda^2}{\lambda^2 - 0.1715^2} + \frac{3.861 \lambda^2}{\lambda^2 - 15.03^2} \quad (1)$$

Aluminum nitride is also a wide bandgap semiconductor material with good electrical insulation and high thermal conductivity, and is able to withstand rapid temperature changes while maintaining stable performance. Aluminum nitride has good chemical resistance to many chemicals and can maintain good performance in different solutions. In addition, its good mechanical strength and high hardness enable it to maintain shape and dimensional stability in the manufacture of optical components. In the optical field, aluminum nitride is transparent to certain wavelengths of light, especially in the ultraviolet and deep ultraviolet regions, which makes it potentially applicable in optical components. The wavelength dependence of the refractive index of aluminum nitride in the wavelength range of 0.22 μm - 5 μm is [19]:

$$n_B^2 = 3.6 + \frac{1.75 \lambda^2}{\lambda^2 - 0.256^2} + \frac{4.1 \lambda^2}{\lambda^2 - 17.86^2} \quad (2)$$

where, n_A and n_B respectively represent the refractive index of gallium nitride and aluminum nitride materials, which λ is the wavelength of the incident light, in the scattering equation, the wavelength is in microns, in other equations, the wavelength is in nanometers. Assume that the thickness of material A, B and C are d_A, d_B, d_C , and their initial values are $d_A = 200 \text{ nm}$, $d_B = 290 \text{ nm}$, $d_C = 440 \text{ nm}$, respectively, and the period number of the structure $N=8$.

In this paper, the empirical equation given in the literature [20] was used to describe the relationship between the concentration of sodium chloride solution and refractive index as follows:

$$S = a_0 + a_1n + a_2n^2 + a_3n^3 + a_4n^4 + a_5n^5 \quad (3)$$

where S denotes the concentration of sodium chloride solution and n denotes the refractive index of sodium chloride solution. According to the empirical formulas given in Table 1, the corresponding refractive index and

defect peak wavelength of sodium chloride solution at different concentrations at 20 °C are included in Table 2 to show the corresponding relationship, so as to more intuitively respond to the influence of the measured concentration on the defect peak wavelength.

Table 1. NaCl solution s - n coefficient of regression

T/°C	a_0	a_1	a_2	a_3	a_4	a_5
10	8249.740	11555.600	-45827.700	29433.300	412.703	-3146.290
20	-121301.00	302045.000	-218058.00	-18068.300	77037.100	-22405.200
30	65519.7000	-83281.200	-86019.400	197641.000	-114658.00	21912.600
40	140501.000	-361504.00	292556.000	-32754.100	-57044.700	18826.400
50	2120.720	-5585.790	2193.360	3068.200	-2481.900	474.788

3. Calculation method

In the sensor designed in this study, we consider one-dimensional Bragg reflection by introducing a defective layer to break its original periodic structure, which leads to a discontinuous electromagnetic wave inside the PBG. When the electromagnetic wave propagates to the sensitive region, different resonance peaks are generated based on different principles such as defects, plasma resonance, and absorption loss. When we change the physical quantity in the sensitive region, the frequency point position of the resonance peaks will also be shifted, and this shift is one-to-one correspondence, which in turn achieves the purpose of identifying the physical quantity. As shown in Fig. 1. The entire surrounding of the structure is placed in air, and TE waves are used for the incident light, which enters the one-dimensional photonic crystal from the air at an angle of incidence θ perpendicular to the sensor.

In this study, we use the transmission matrix method to investigate the interaction between each layer of the structure, which can be described by equation (4) for media A, B, C [21]:

$$M_j = \begin{pmatrix} \cos(k_{jx}d_j) & -\frac{i}{\eta_j} \sin(k_{jx}d_j) \\ -i\eta_j \sin(k_{jx}d_j) & \cos(k_{jx}d_j) \end{pmatrix} \quad (4)$$

where $j=A, B, C, k_{jx} = \frac{2\pi n_j \cos \theta_j}{\lambda}$ stand the wave vector in the x direction. d_j Represents the thickness of the j -layer. $\eta_j = n_j \cos(k_{jx}d_j)$ stands the refractive index of layer j .

For the interaction between each layer of material, it can be described by the total transport matrix, which is shown in equation (5):

$$M = (M_A M_B)^N M_C (M_B M_A)^N = \begin{pmatrix} M_{11} & M_{12} \\ M_{21} & M_{22} \end{pmatrix} \quad (5)$$

The transmission coefficient is calculated as in equation (6):

$$t = \frac{2q_0}{(M_{11} + M_{12}q_s)q_0 + (M_{21} + M_{22}q_s)} \quad (6)$$

The equations $q_0 = n_0 \cos \theta$ and $q_s = n_s \cos \theta$ denote the phase difference of the TE polarization wave associated with the light wave in the incoming and outgoing media, respectively. The transmittance of our designed sensor can then be calculated using equation (7):

$$T = \frac{q_s}{q_0} |t|^2 \quad (7)$$

4. Results and discussion

Fig. 2 represents the dispersion diagrams of Gallium Nitride and Aluminum Nitride in the wavelength range of 800 nm-1200 nm, from which it can be seen that the refractive indices of Gallium Nitride and Aluminum Nitride show a decreasing trend as the wavelength increases. However, the effect of electromagnetic waves in the wavelength range of 800 nm-1200 nm on the refractive index of the two materials is limited, and in this interval, the value of the change in the refractive index of Gallium Nitride is 0.004, and the value of the change in the refractive index of Aluminum Nitride is 0.01, which indicates that Aluminum Nitride is more sensitive to the electromagnetic waves in this interval.

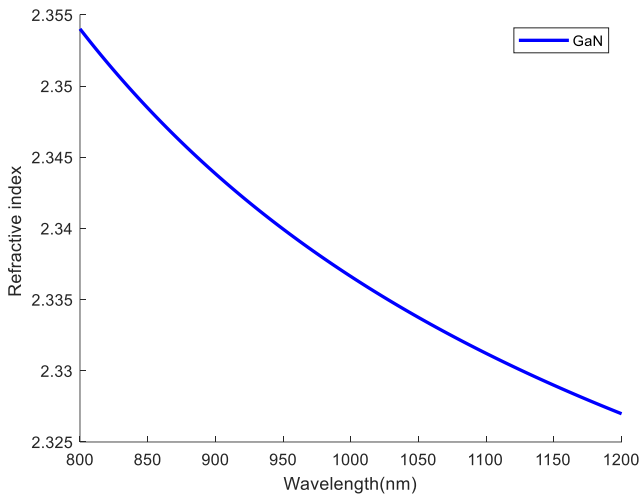


Fig. 2a. GaN refractive index as a function of wavelength

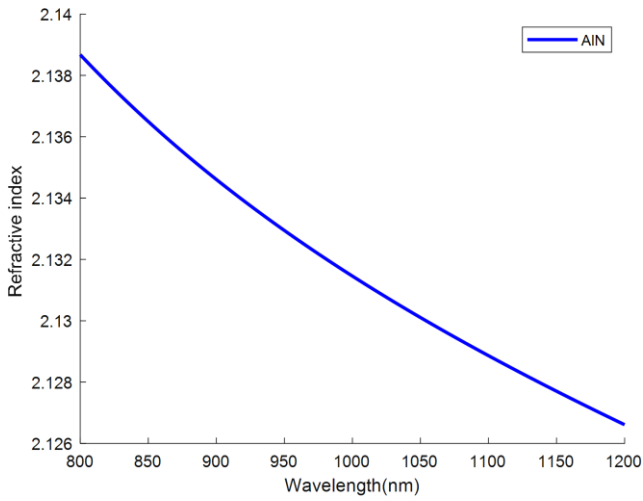


Fig. 2b. AlN refractive index as a function of wavelength

Fig. 3 shows the transmission spectra of the structure when no defects were introduced. In the initial structure, the wavelength range of the incident electromagnetic wave is 800 nm - 1200 nm, which is mainly in the near-infrared band. By observing the transmission spectrogram, it can be seen that when the wavelength of the electromagnetic wave is between 960 nm - 1060 nm, the transmittance is almost zero, which indicates that electromagnetic waves in this wavelength range cannot pass through the structure, forming a good photon forbidden band. The original periodic structure was broken when we introduced a cavity layer C of a water sample with a refractive index of 1.33 as a defect in the structure. This defect introduces a passband in the PBG, which forms a sharp transmission peak (TP), and the results are shown in Fig. 4. The wavelength of the transmission peak is localized at 994.446 nm, and the transmittance is as high as 0.98, which means that the structure has a very high transmittance of light at this particular wavelength. This phenomenon can be explained by the introduction of defects in the structure

leading to the localization of photons, which results in enhanced transmission of light of a specific wavelength in the structure.

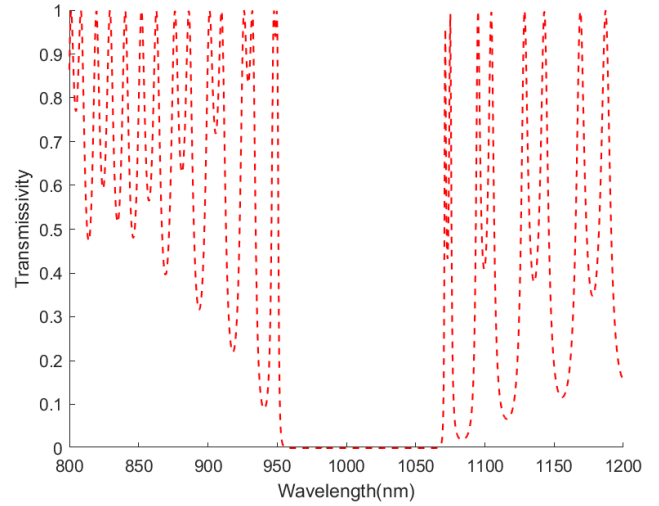


Fig. 3. Transmissivity rate map without defects introduced

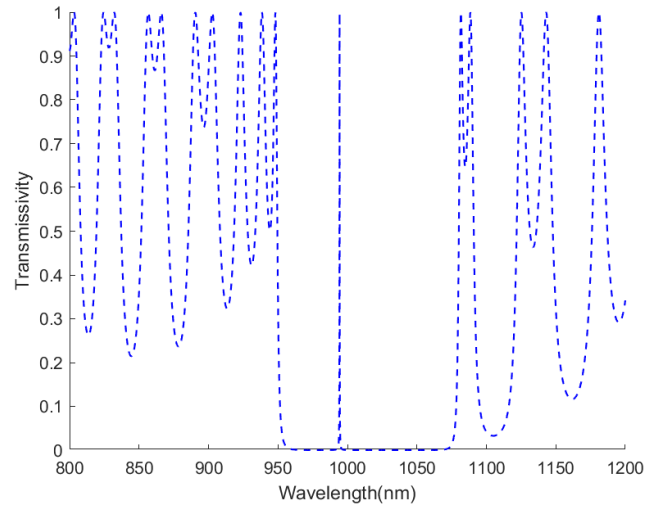


Fig. 4. Transmissivity rate map with defects introduced

We added sodium chloride solutions with concentrations of 4%, 8%, 12%, 16%, 20%, 24%, 28%, and 32% to the cavity layer and observed significant changes in the transmission spectra. Fig. 5 illustrates the transmission spectra plots of different concentrations of sodium chloride solutions for these experiments, which were performed at a controlled external temperature of 20 °C. It can be seen from Fig. 5 that the transmission electromagnetic wave shifts towards longer wavelengths as the concentration of sodium chloride solution increases at 20 °C. The reason for the shift in the transmission peak wavelength is that when the concentration of sodium chloride in the solution increases, it leads to a subsequent increase in the refractive index of the solution. This increased refractive index affects the speed and path of light propagating

through the structure, and the optical thickness corresponding to the defective layer increases, which in

turn changes the features in the transmission spectrum.

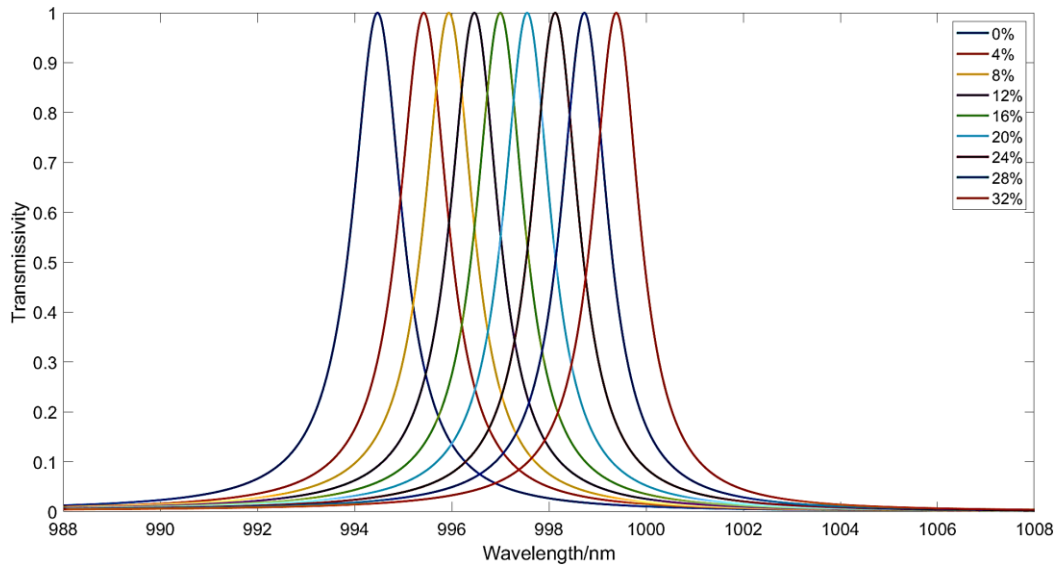


Fig. 5. Transmissivity spectra corresponding to solution of different concentrations of sodium chloride (colour online)

The change in the concentration of the sodium chloride solution resulted in the shift of the transmission peak. In order to better reflect the shift of the transmission peak wavelength in relation to the sodium chloride solution, we investigated the relationship between the incident wavelength and the refractive index of the solution, and we can clearly see from Fig. 6 that when the refractive index of the sodium chloride solution is in the interval of 1.3-1.4, the incident wavelength and the refractive index of the solution maintain a very good linear relationship, and the linearity and linear range are more prominent.

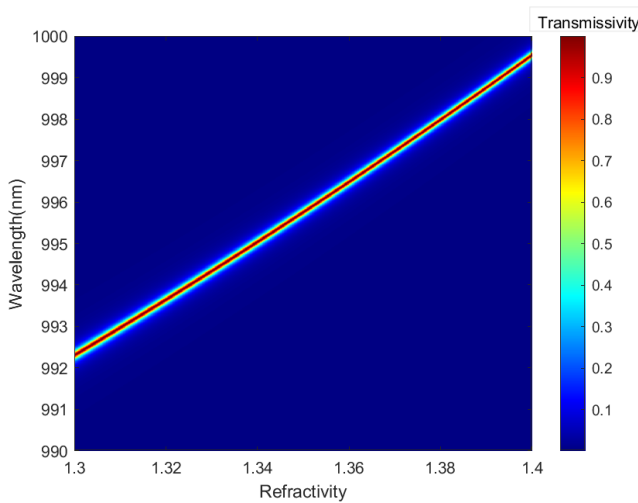


Fig. 6. Top view of transmittance corresponding to changes in refractive index (colour online)

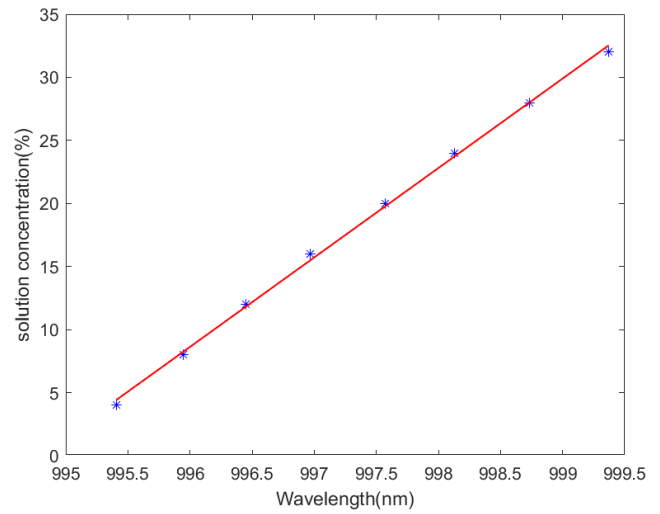


Fig. 7. The linear relationship between wavelength and solution concentration

Table 2. Refractive index to different concentrations of sodium chloride solution at 20 °C

NaCl solution concentration $S/\%$	Refractive index of solution n/RIU
4	1.3433
8	1.3504
12	1.3575
16	1.3646
20	1.3719
24	1.3794
28	1.3871
32	1.3954

In order to further obtain the relationship between the concentration of sodium chloride solution and the transmission peak wavelength, we extracted the transmission peak wavelengths of sodium chloride solutions with concentrations of 4%, 8%, 12%, 16%, 20%, 24%, 28%, and 32%, respectively, and combined with the data given in Table 2, we performed a first-order linear fit between the concentration of sodium chloride solution and the transmission peak wavelengths, and the results are shown in Fig. 7. From Fig. 7, it can be seen that the transmission peak wavelength is proportional to the concentration of sodium chloride solution, and the first-order linear fitting equation of the transmission peak wavelength to the concentration of sodium chloride solution is:

$$S = \frac{7.0921\lambda - 7055.0897}{100} \times 100\% \quad , \quad \text{linearity}$$

$R^2 = 0.9986$. The sensitivity of the transmission peak wavelength as a function of solution concentration [22]:

$$S_1 = \frac{\Delta\lambda}{\Delta n} = 1002 \text{ nm} / \text{RIU} (20.8 \text{ nm} / \%) \quad (8)$$

Our proposed structure has high sensitivity in sodium chloride solution concentration measurement compared to existing measurement methods. By detecting the peak wavelength of the transmission peak of the one-dimensional photonic crystal sensing model, the corresponding concentration value can be accurately obtained. This method has high detection sensitivity and can quickly and accurately realize the monitoring of sodium chloride solution concentration.

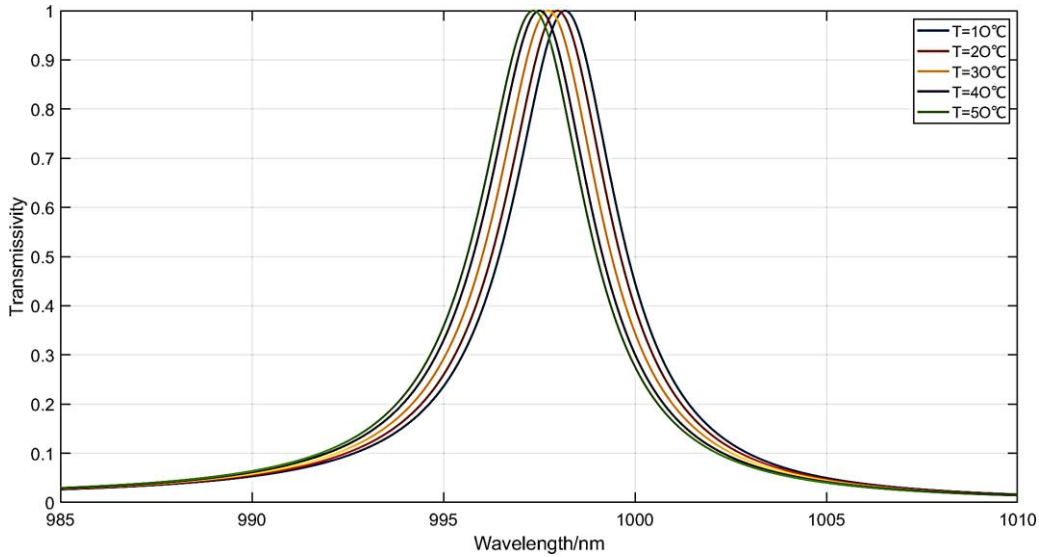


Fig. 8. Transmission spectra of solutions at different temperatures (colour online)

Since temperature affects the refractive index of sodium chloride solution, we investigated the effect of temperature on the sensor. We configured a standard sodium chloride solution with a concentration of 16%, and according to Table 1 we calculated the refractive indices of the solution under different temperature conditions, and injected it into the defective layer of the photonic crystal model for transmission spectrum simulation test. The transmission spectra of the photonic crystal when the temperatures were 10 °C, 20 °C, 30 °C, 40 °C, and 50 °C are shown in Fig. 8, from which it can be seen that the wavelength of the defect peaks shifted to the short-wave direction with the increase of the temperature, which is due to the fact that the effective refractive index of the NaCl solution decreases when the temperature increases. We extracted the transmission peak wavelengths at different temperatures and calculated the sensitivity of the transmission peak wavelength shift with temperature:

$$S_2 = \frac{\Delta\lambda}{\Delta T} = 0.02 \text{ nm}/^\circ\text{C} \quad (9)$$

This is a very small sensitivity, indicating that the sensor we designed is not sensitive to changes in temperature. Compared with the change in the wavelength of the transmission peak due to the change in the concentration of the sodium chloride solution, the effect of the change in ambient temperature on the measurement results is very small, and the measurement results have good stability.

The period number of the photonic crystal directly determines the size and fabrication cost of the sensor, so we investigated the effect of different period numbers on the photonic bandgap and how to optimize the response of the sensor to specific wavelengths of light by adjusting the period. Keeping the same number of cycles before and after the defect layer, the cycle number N is taken as

5, 6, 7 and 8, respectively, and other simulation parameters remain unchanged, Fig. 9 shows the transmittance of the photonic crystal under different cycle numbers, from which it can be seen that, when the cycle number N of the photonic crystal is increased sequentially from 5 to 8, the energy bandwidth of the photonic crystal is not shifted significantly, and is still kept in the range of the interval of 960 nm to 1060 nm. The transmitted electromagnetic waves outside the photonic forbidden band range are obviously shifted, while the wavelength of the transmission peaks located in the forbidden band range does not move significantly, and the transmittance does not change with the increase of the number of cycles and always stays at the high level of 0.9 or above.

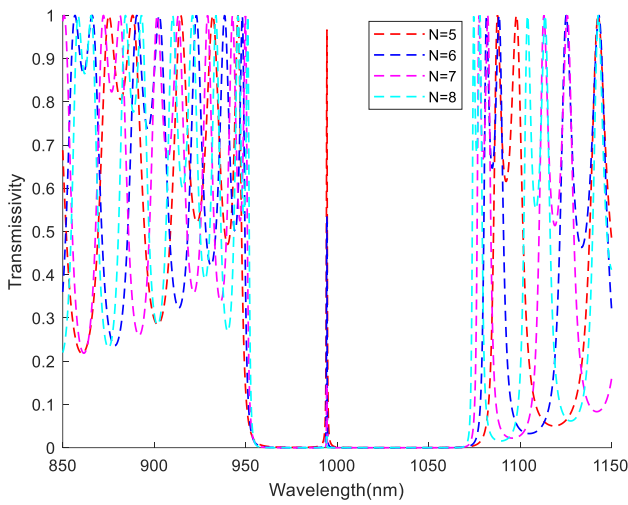


Fig. 9. Transmission spectra at different period numbers (colour online)

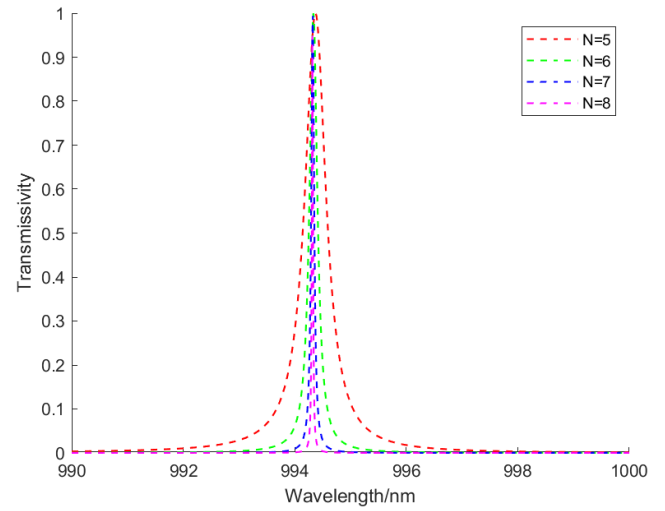


Fig. 10. The effect of the number of periods on the TP (colour online)

In order to understand more accurately the effect of the period number N on the transmission peaks in the photon forbidden band range, we plotted the transmission peaks at different period numbers, and it can be seen from Fig. 10 that the transmission peaks become sharper as the period number N increases from 5 to 8. When $N=5$, the quality factor $Q=248$; when $N=6$, $Q=500$; when $N=7$, $Q=1100$; when $N=8$, $Q=1990$. Therefore, as the number of cycles N increases, it means higher quality factor and higher detection sensitivity of the transmission peak. Therefore, by carefully designing the period number of the photonic crystal, the characteristics of the transmission peak can be effectively controlled, thus improving the accuracy and reliability of the measurement.

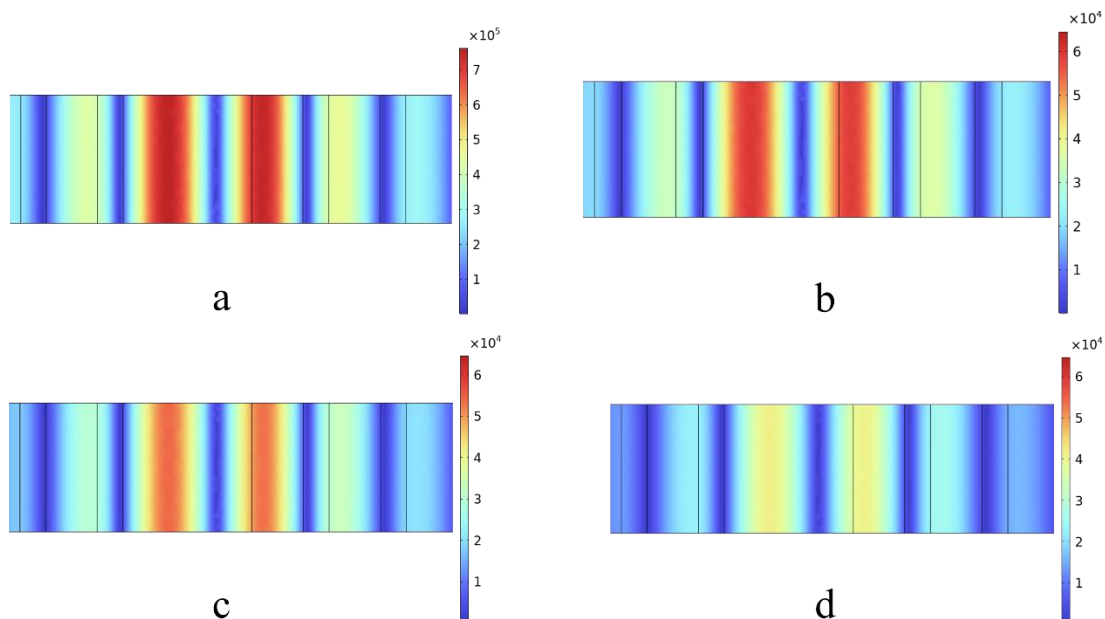


Fig. 11. Electric field distribution in defective layer at different incidence angles (color online)

a. $\theta=0^\circ$, b. $\theta=10^\circ$, c. $\theta=20^\circ$, d. $\theta=40^\circ$ (colour online)

The variation of the incidence angle is also an important factor affecting the performance of the photonic crystal, we will determine the optimal incidence angle by simulating the light transport properties at different incidence angles to achieve the maximum photon localization and the strongest light-matter interaction. Keeping other parameters unchanged, the incidence angle Θ is selected as 0° , 10° , 20° , and 30° in order, and the electric field strength at the center of the defect layer is simulated. Fig. 11 demonstrates the electric field distribution in the defect layer at different incidence angles, as can be seen from the figure, with the increase of incidence angle, the electric field strength in the center of the defective layer gradually weakened, and the electric field strength decreased from the initial

7×10^5 V/m to 4×10^4 V/m. With the weakening of the electric field strength at the defective layer, the interaction between the electromagnetic wave and the NaCl solution was also weakened, and the electromagnetic wave that passes through the photonic crystal was reduced, which led to the decrease of the transmittance of the transmission peak. In order to maintain a high transmittance, we chose the vertical incidence ($\Theta=0$) for the measurement. We have analyzed the structure, analyte, sensitivity, and quality factor of this sensor in comparison with the sensor models proposed by other researchers, and the results are shown in Table 3, from which we can see that our proposed sensor model from the sensor model performs much better in terms of sensitivity and quality factor.

Table 3. Comparison of the performance of this sensing model with other sensing models

Year	Structure	Analytes	S(nm/RIU)	QF	References
2021	coupling topology	index of refraction	550	304	[23]
2022	2Dpc	Red blood cells	898	212	[24]
2022	coupling topology	Basal cell cancer	718	156	[14]
2024	1Dpc	Blood	1074	468	[25]
Our work	1Dpc	NaCl solution	1002	1990	-

5. Conclusion

We propose a one-dimensional mirror photonic crystal sensing model based on gallium nitride and aluminum nitride, which enables efficient, real-time detection of sodium chloride solution concentration. The sensor has good stability and is less affected by the ambient temperature. By investigating the effects of the number of photonic crystal periods and the incident angle on the sensor, the results show that the model has the highest quality factor of 1990 when the number of periods $N=8$, and the highest transmittance when the incident angle is 0° . Finally, we analyze the sensor model proposed in this study in comparison with other reports, which has more outstanding performance in sensitivity and quality factor.

References

- [1] S. John, Phys. Rev. Lett. **58**(23), 2486 (1987).
- [2] E. Yablonovitch, Phys. Rev. Lett. **58**(20), 2059 (1987).
- [3] G. J. Tang, X. T. He, F. L. Shi, J. W. Liu, X. D. Chen, J. W. Dong, Laser Photonics Rev. **16**(4), 2100300 (2022).
- [4] O. Painter, J. Vučković, A. Scherer, J. Opt. Soc. Am. B **16**(2), 275 (1999).
- [5] A. H. Aly, H. A. Elsayed, Physica B **407**(1), 120 (2012).
- [6] L. Qi, Z. Yang, T. Fu, Phys. Plasmas **19**(1), 012509 (2012).
- [7] R. D. Meade, K. D. Brommer, A. M. Rappe, J. D. Joannopoulos, Phys. Rev. B **44**(19), 10961 (1991).
- [8] E. Moreno, F. J. García-Vidal, L. Martín-Moreno, Phys. Rev. B **69**(12), 121402 (2004).
- [9] V. N. Konopsky, E. V. Alieva, Anal. Chem. **79**(12), 4729 (2007).
- [10] Z. A. Zaky, M. Mohaseb, A. Panda, H. A. Amer, A. M. Farag, J. Kovac, P. D. Pukhrabam, V. Dhasarathan, A. H. Aly, Opt. Quant. Electron. **55**(7), 584 (2023).
- [11] B. F. Wan, Y. Xu, Z. W. Zhou, D. Zhang, H. F. Zhang, IEEE Sens. J. **21**(3), 2846 (2020).
- [12] A. H. Aly, B. A. Mohamed, S. K. Awasthi, S. A. O. Abdallah, A. F. Amin, Sci. Rep. **13**(1), 9422 (2023).
- [13] Z. A. Zaky, M. A. Mohaseb, A. Panda, H. A. Amer, A. M. Farag, J. Kovac, P. D. Pukhrabam, V. Dhasarathan, A. H. Aly, Opt. Quant. Electron. **55**(7), 584 (2023).
- [14] S. Khani, M. Hayati. Sci. Rep. **12**(1), 5246 (2022).
- [15] A. Panda, P. D. Pukhrabam, G. Keiser, Microsyst. Technol. **27**, 833 (2021).
- [16] S. Lin, H. Zhao, L. Zhu, T. He, S. Chen, C. Gao, L.

- Zhang, *Desalination* **498**, 114728 (2021).
- [17] Z. You, Y. Lai, H. Zeng, Y. Yang, *Constr. Build. Mater.* **238**, 117762 (2020).
- [18] A. S. Barker Jr, M. Ilegems, *Phys. Rev. B* **7**, 743 (1973).
- [19] J. Pastrňák, L. *Phys. Stat. Sol.* **14**, K5-K8 (1966).
- [20] M. Born, E. Wolf, *Principles Opt.* **44**, 1 (1980).
- [21] Y. Mei, F. Zhu, J. Zhuang, *Electronic Measurement Technology* **45**(24), 54 (2022).
- [22] Y. Mei, F. H. Zhu, J. J. Zhuang, *Electronic Measurement Technology* **45**(24), 54 (2022).
- [23] S. Khani, M. Hayati, *Superlattices Microstruct.* **156**, 106970 (2021).
- [24] A. Rashidnia, H. Pakarzadeh, M. Hatami, N. Ayyanar, *Opt. Quant. Electron.* **54**, 38 (2022).
- [25] B. Ankita, Suthar, S. Bissa, A. Bhargava, *Opt. Quant. Electron.* **56**(7), 1116 (2024).

*Corresponding author: jwwu@cqu.edu.cn